Blood Flow Regulation by *S*-Nitrosohemoglobin in the Physiological Oxygen Gradient

Jonathan S. Stamler,* Li Jia, Jerry P. Eu, Timothy J. McMahon, Ivan T. Demchenko, Joseph Bonaventura, Kim Gernert, Claude A. Piantadosi

The binding of oxygen to heme irons in hemoglobin promotes the binding of nitric oxide (NO) to cysteineβ93, forming *S*-nitrosohemoglobin. Deoxygenation is accompanied by an allosteric transition in *S*-nitrosohemoglobin [from the R (oxygenated) to the T (deoxygenated) structure] that releases the NO group. *S*-nitrosohemoglobin contracts blood vessels and decreases cerebral perfusion in the R structure and relaxes vessels to improve blood flow in the T structure. By thus sensing the physiological oxygen gradient in tissues, hemoglobin exploits conformation-associated changes in the position of cysteineβ93 SNO to bring local blood flow into line with oxygen requirements.

Hemoglobin (Hb) is the tetrameric protein in red blood cells (RBCs) that transports oxygen (O_2) from the lung to the tissues (*1*). As RBCs saturated in O_2 migrate through small arteries and resistance arterioles, they are exposed to an O_2 gradient (*2*). By the time Hb reaches the capillaries, a large fraction (~50 to 65%) of the O_2 has been lost to venous exchange (a functional shunt) (*2*). Only about 25 to 30% of the O_2 is extracted by the tissues to meet basal metabolic requirements (*1–3*). Exposed to increasing oxygen tension (PO_2) in postcapillary venules and veins (*2*), Hb is ~75% saturated in O_2 (*1, 3*) upon entering the lung. Thus, on average, only one of four O_2 molecules carried by Hb is used in the respiratory cycle, even though extensive deoxygenation occurs in the flow-controlling resistance vessels.

Hemoglobin exists in two alternative structures, named R (for relaxed, high O_2 affinity) and T (for tense, low O_2 affinity) (*4*). Hemoglobin assumes the T structure to efficiently release O_2 (*4*). The allosteric transition in Hb (from R to T) controls the reactivity of two highly conserved cysteines (Cysβ93) that can react with NO or SNO (*S*-nitrosothiol) (*5*). Thiol affinity for (S)NO is high in the R structure and low in the T structure. In other words, the NO group is released from thiols of Hb in low PO_2 (*5*). A major function of (S)NO in the vasculature is to regulate blood flow, which is controlled by the resistance arterioles (*6*). We therefore proposed that partial deoxygenation of SNO-Hb in these vessels might actually promote O_2 delivery by liberating (S)NO. That is, the allosteric transition in Hb would function to release (S)NO in order to increase blood flow.

Hemoglobin is mainly in the R (oxy) structure in both 95% O_2 and 21% O_2 (room air) (*4*). Hb and SNO-Hb both contract blood vessels in bioassays (*7*) at these O_2 concentrations (Fig. 1A). That is, their hemes sequester NO from the endothelium. In hypoxia [<1% O_2 (at a simulated tissue PO_2 of ~6 mmHg)], which promotes the T structure (*4*), Hb strongly contracts blood vessels, whereas SNO-Hb does not (Fig. 1B). NO group release from SNO-Hb is accelerated in RBCs by glutathione (*5*), which enhances SNO-Hb relaxations through formation of *S*-nitrosoglutathione (GSNO) (Fig. 1C). The potentiation by glutathione is inversely related to the PO_2 (Fig. 1C), because NO group transfer from SNO-Hb is promoted in the T structure (*5*). In contrast, relaxations by GSNO are largely independent of PO_2 (Fig. 1D) and are unmodified by superoxide dismutase (*8*). Thus, in the T structure, relaxation by SNO overwhelms the contraction caused by NO scavenging at the heme, whereas the opposite is true in R. Red blood cells containing SNO-Hb (SNO-RBCs) (*5*) function in vessel ring bioassays like cell-free SNO-Hb (*9*).

The molecular basis for the structure-function relations of SNO-Hb was examined in the crystal structures of oxy and deoxy Hb and in models of Cysβ93 SNO (*10*). The results indicate that Cysβ93 assumes positions in deoxy Hb and oxy Hb that dictate the reactivity of the thiol. In deoxy Hb, Cysβ93 points out toward the protein surface, up above the external His^{146}-Asp^{94} salt bridge. The γ sulfur of Cysβ93 is deactivated by the salt bridge that shields it and the acidic milieu of Asp^{94}/Glu^{90}, which maintains its protonation (Fig. 2A). Thus, in the T structure, thiol reactivity toward NO-related species is low (*5*). In oxy Hb, the salt bridge breaks and Cysβ93 points in and away from solvent (Fig. 2B). The Cysβ93 is brought into proximity with Hisβ92, which would be expected to facilitate deprotonation of the sulfur and enhance its nucleophilicity. Thus *S*-nitrosylation is facilitated in the R structure (*5*). Further modeling showed that the

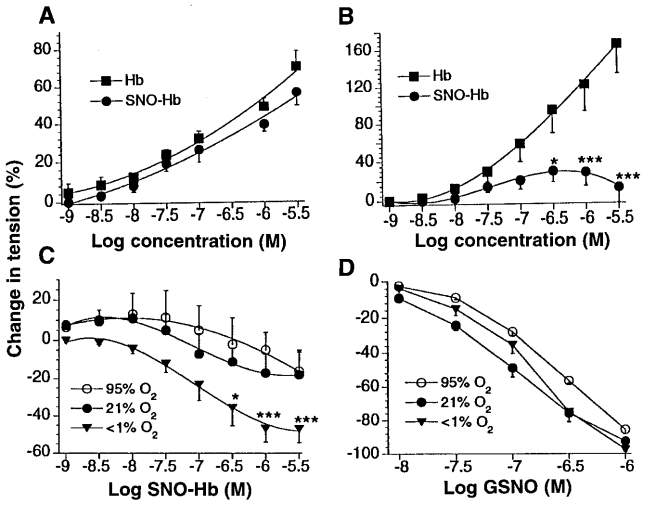

Fig. 1. Oxygen-dependent vasoactivity of SNO-Hb. (**A**) Effects of oxy Hb and SNO–oxy Hb in 95% O_2 (the R structure) on tension in rabbit thoracic aorta as measured in ring bioassays (*7*). Curves are not different by analysis of variance (ANOVA); $n = 12$ for each data point. Similar responses were seen with 50 μM SNO–oxy Hb/oxy Hb and in 21% O_2. (**B**) Effect of deoxy Hb and SNO–deoxy Hb in <1% O_2 (~6 torr) (the T structure). Responses of SNO-Hb and Hb are significantly different. (In most experiments, SNO-Hb caused a small degree of contraction at lower doses and initiated relaxations at the highest dose; in some experiments, it caused dose-dependent relaxations.) $n = 13$ for each data point; $^*P < 0.05$; $^{***}P < 0.001$ by ANOVA. (**C**) Potentiation of SNO-Hb vasorelaxation by 10 μM glutathione is dependent on O_2 concentration. The curve for <1% O_2 is statistically different from both 95 and 21% O_2 ($P < 0.001$), which are not different from one another by ANOVA ($n = 6$ for all data points). Glutathione (10 μM) has no effect on native Hb contractions. (**D**) Vasorelaxant effects of GSNO are unaffected by O_2 concentration; $n = 6$ for each point. Methods are described in (*7*).

J. S. Stamler, Department of Medicine, Divisions of Respiratory and Cardiovascular Medicine and Department of Cell Biology, Duke University Medical Center, Room 321 MSRB, Box 2612, Durham, NC 27710, USA.
L. Jia, J. P. Eu, T. J. McMahon, I. T. Demchenko, C. A. Piantadosi, Department of Medicine, Division of Respiratory Medicine, Duke University Medical Center, Durham, NC 27710, USA.
J. Bonaventura, Department of Cell Biology and Nicholas School of the Environment, Duke University Medical Center, Durham, NC 27710, USA.
K. Gernert, Department of Biochemistry, Duke University Medical Center, Durham, NC 27710, USA.
*To whom correspondence should be addressed.

NO group may only be released in the T structure. In deoxy SNO-Hb, the SNO is positioned out toward the aqueous phase, either above or below the intact His^{146}-Asp^{94} salt bridge (Fig. 2C), making both the S and the N readily exposed to solvent. In contrast, the NO group points toward the back side of the heme and away from solvent in the oxy structure (Fig. 2D). Although the salt bridge is broken, the SNO is completely buried. Accordingly, the Cysβ93 SNO is likely to be reactive (and thus a good NO donor) in the T or deoxy conformation and unreactive (hence a poor NO donor) in the R or oxy conformation.

Allosteric control of SNO-Hb by O_2 was assessed in rats (*11*). The periarteriolar O_2 gradient [the artery-arteriole and arterial-venous (A-V) difference in Hb O_2 saturation] was eliminated in hyperbaric chambers by application of 3 atm of absolute pressure (ATA) while the animals breathed 100% O_2 (*12*). We then measured the levels of SNO-Hb and nitrosyl Hb (Hb[Fe]NO) in blood that perfuses the brain. As reported previously (*5*), venous blood (21% O_2) contained mostly nitrosyl Hb, whereas arterial blood contained significant amounts of SNO-Hb (Fig. 3). On the other hand, SNO-Hb predominated in both arterial and venous blood in 100% O_2 plus 3 ATA (Fig. 3). We conclude that (i) SNO-Hb appears to form endogenously in the R structure, whereas SNO is released in the T structure [compare arterial 100% O_2 plus 3 ATA (R state) with venous 21% O_2 (T state)]; (ii) binding of NO to hemes of Hb is favored in the T structure; indeed, some of the NO released during A-V transit appears to be autocaptured at the hemes; and (iii) maintaining endogenous SNO-Hb in the R structure by eliminating the A-V O_2 gradient preserves levels of SNO (compare arterial 21% O_2 with venous 100% O_2 plus 3 ATA). Thus, SNO-Hb should increase cerebral blood flow in 21% O_2 when SNO is readily released during A-V transit but not under the hyperoxic conditions that maintain the R structure in the artery and vein.

The cerebrovascular effects of SNO-Hb were measured in Sprague-Dawley rats with O_2 and H_2 (blood flow)–sensitive microelectrodes that were placed stereotaxically in several regions of the brain (*11*). Tissue/microvascular PO_2 ranged from 19 to 37 mmHg in 21% O_2, from 68 to 138 mmHg in 100% O_2, and from 365 to 538 mmHg in 100% O_2 plus 3 ATA. SNO-Hb increased cerebral blood flow in rats inspiring 21% O_2 (that is, it appropriately increased blood flow in relatively hypoxic tissues) (Fig. 4). The increase in local blood flow in all regions of the brain was attenuated in 100% O_2 (Fig. 4) and changed, appropriately, to decreases in flow in 100% O_2 plus 3 ATA (Fig. 4). Neither Hb, which paradoxically decreased blood flow to hypoxic tissues (Fig. 4), nor GSNO, which increased blood flow even to hyperoxic tissues (*8*), exhibited O_2-dependent effects.

Figure 5 shows the effects of SNO–oxy Hb, oxy Hb, and GSNO on blood pressure in animals breathing 21% O_2 or 100% O_2 (*11*). Hb produced increases in blood pres-

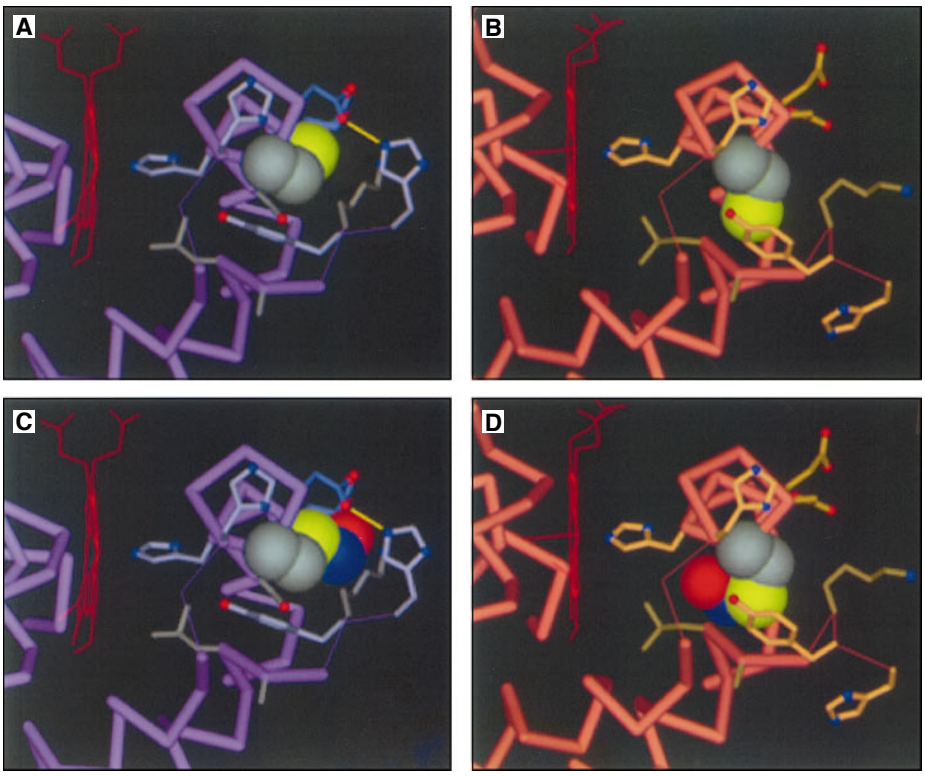

Fig. 2. Structural models of Hb and SNO-Hb: R- and T-dependent positioning of Cysβ93 and Cysβ93 SNO. (**A**) Deoxy Hb. Cysβ93 points out toward the protein surface, up above the external His^{146}-Asp^{94} salt bridge; Tyrβ145 packs alongside its side chain. The γ sulfur of Cysβ93 (yellow) is accessible to solvent in a cavity formed by the COOH-terminus of β helix F, the COOH-terminus of the β subunit, and helix C of the α2 subunit. There is no significant difference between the flexibility of Cysβ93 and the β subunit backbone (as measured by crystal temperature factors), which suggests that the position of Cysβ93 is real and stable. The α and β carbons of Cysβ93 are gray. (**B**) Oxy Hb. Cysβ93 points in and away from solvent (and the broken salt bridge); Tyrβ145 is positioned over the top of its side chain. The γ sulfur of Cysβ93 is buried below its β carbon (gray) and is further shielded by structural changes. As in deoxy Hb, the position of Cysβ93 is rigid, greatly increasing confidence that the conformational differences in the position of Cysβ93 are real. (**C**) SNO-deoxy Hb. In the T structure, SNO is highly exposed to solvent (that is, able to donate NO), being positioned either above or below the His^{146}-Asp^{94} salt bridge. If positioned up, the sulfur (yellow) and nitrogen (blue) are exposed. If positioned down, the sulfur and oxygen (red) are exposed. (**D**) SNO-oxy Hb. In the R structure, SNO is highly protected from solvent (that is, unable to donate NO). The NO group (blue and red) is accommodated toward the back side of the β heme, under Tyrβ145. The β carbon (gray) buries the sulfur (yellow). The SNO is also shielded by the backbone and side-chain conformations. SNO can assume only a few positions without van der Waals overlaps in the R structure.

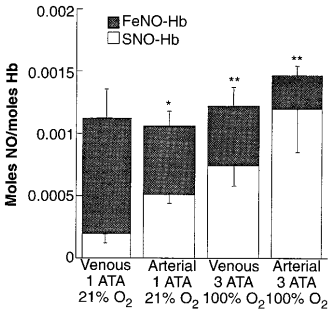

Fig. 3. Influence of O_2 tension on endogenous levels of SNO-Hb and nitrosyl hemoglobin (FeNO-Hb). Blood was drawn from indwelling catheters in the carotid artery (arterial) and superior vena cava/right atrium (venous) of five rats exposed first to room air (21% O_2) and then 100% O_2 + 3 ATA in a hyperbaric chamber. The mean O_2 saturation of venous blood (room air) was 69%; of arterial blood (room air), it was 93%; of venous blood (100% + 3 ATA), it was also 93%; and of arterial blood (100% + 3 ATA), it was 100%. *FeNO-Hb venous 21% O_2 versus arterial 21% O_2, $P = 0.008$; **SNO-Hb (venous or arterial) 100% O_2 + 3 ATA versus venous 21% O_2, $P \leq 0.004$. SNO-Hb and FeNO-Hb were not statistically different in artery 21% O_2 versus venous 100% + 3 ATA (which have identical O_2 saturations), nor in venous versus arterial 100% O_2 + 3 ATA. Methods are described in (*5*) and (*11*).

sure that were significantly greater than those produced by SNO-Hb, whereas GSNO lowered blood pressure. Infusions of SNO-RBCs also lowered blood pressure in a manner consistent with a GSNO-like effect (*13*). The effects of SNO-Hb and Hb on blood pressure suggest that SNO is released in resistance arterioles to compensate for NO scavenging at the heme irons.

Oxygen delivery to tissues is a function of the O_2 content of blood and blood flow (*14*). Blood oxygen content is largely determined by Hb, which undergoes allosteric transitions in the lung and systemic microvasculature that promote the binding and release of O_2 (*1*, *4*). Regional blood flow is regulated by the metabolic requirements of the tissue: Blood flow is increased by hypoxia and decreased when O_2 supply exceeds demand (*6*). These classical physiological responses are thought to be partly mediated by changes in the level of endothelial-derived NO (*15*).

This standard picture has some problems. First, it is unclear why O_2 is lost to (countercurrent) venous exchange before reaching the tissues (*2*). Second, RBCs seem to oppose their own O_2 delivery function. Specifically, Hb reduces blood flow and blunts hypoxic vasodilation by sequestering NO in terminal arterioles and capillaries (*16*) (note in vivo effects of Hb in Fig. 4). Our finding that the O_2 gradient (low PO_2) in precapillary resistance vessels promotes NO group release from SNO-Hb resolves these paradoxes. That is, SNO-Hb compensates for NO scavenging at the heme iron by assuming the T structure, which liberates (S)NO. Stated another way, SNO-Hb senses the tissue PO_2 and then uses the allosteric transition as a way to control arteriolar tone. If the tissue is hypoxic, SNO is released to improve blood flow. However, if O_2 supply exceeds demand, SNO-Hb retains the NO group by maintaining the R structure—with the net effect of reducing blood flow in line with demand. We suggest that SNO-Hb contributes to the classical physiological responses of hypoxic vasodilation and hyperoxic vasoconstriction.

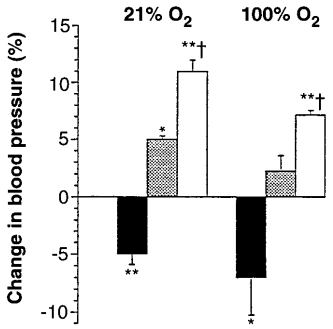

Fig. 5. Hemodynamics of SNO-Hb (gray bars), Hb (white bars), and GSNO (black bars) at different O_2 concentrations. SNO-Hb produced significantly less of an increase in blood pressure than did Hb ($P < 0.05$), whereas GSNO decreased blood pressure. $n = 5$ to 6 for each drug; $^*P < 0.05$, $^{**}P < 0.01$ versus baseline blood pressure; †$P < 0.05$ versus SNO-Hb. Drugs were infused through the femoral vein at 1 μmol/kg over 1 min after blood pressure had stabilized (approximately 30 min) (*5*). Measurements shown were taken at 10 min after infusion of the drug. Similar responses were seen at 3 and 20 min.

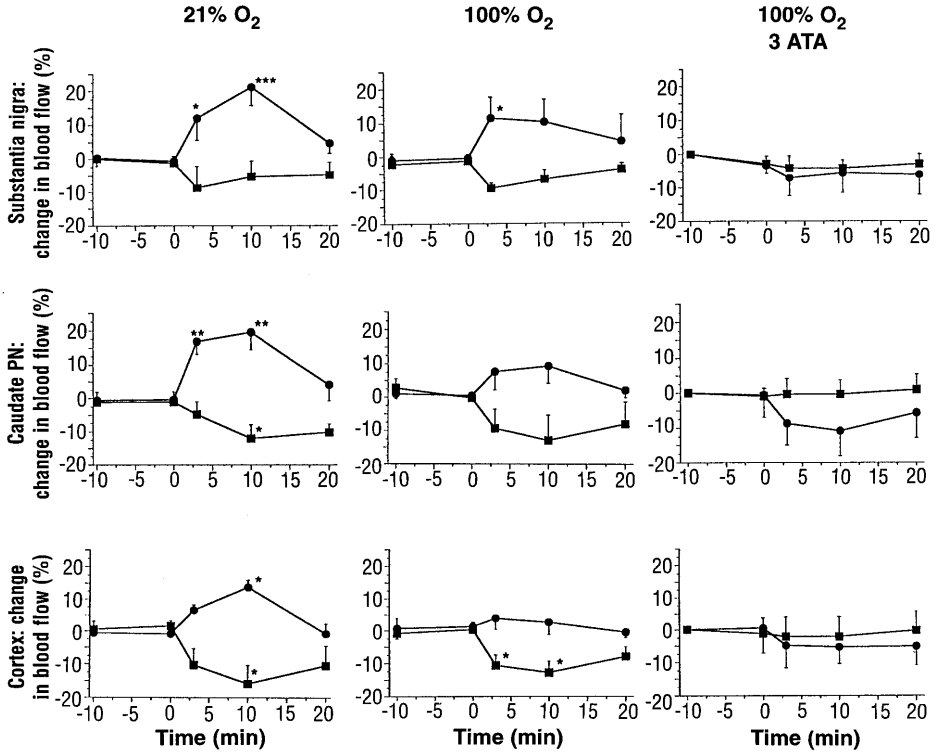

Fig. 4. Oxygen-dependent effects of SNO-Hb and Hb on local cerebral blood flow. Comparative effects of SNO-Hb (circles) and Hb (squares) (1 μmol/kg infused over 3 min) on local blood flow in the substantia nigra, caudate putamen nucleus (caudate PN), and parietal cortex are shown across the physiological oxygen gradient. In 21% O_2, all curves are statistically significantly different from one another and from baseline by ANOVA. In 100% O_2, the increase in flow to SNO-Hb was significantly attenuated (only the SN increase reached statistical significance), but the Hb-mediated decrease in flow was preserved (all curves remain different from one another by ANOVA to $P < 0.05$). In 100% O_2 + 3 ATA, curves are not different by ANOVA. Baseline blood flow was decreased by ~10% under 100% O_2 + 3 ATA as compared with 100% O_2. $n = 7$ for all data points.

We envision the following picture. Partially nitrosylated Hb (Hb[FeII]NO) enters the lung in the T structure. There, *S*-nitrosylation is facilitated by the O_2-induced conformational change in Hb. SNO–oxy Hb (SNO-Hb[FeII]O_2) enters the systemic circulation in the R structure. Oxygen losses in precapillary resistance vessels then effect an allosteric transition (from R to T) in Hb, which liberates (S)NO to dilate blood vessels. NO released from Hb may be transferred directly to the endothelium or by way of low-mass *S*-nitrosothiols such as GSNO, which are exported from RBCs (*5*). Thus, the O_2 gradient in arterioles serves to enhance O_2 delivery: It promotes an allosteric transition in Hb which releases (S)NO to improve blood flow.

REFERENCES AND NOTES

1. L. Stryer, in *Biochemistry*, L. Stryer, Ed. (Freeman, San Francisco, CA, 1981), pp. 43–82; A. C. Guyton, in *Textbook of Medical Physiology* (Saunders, Philadelphia, PA, 1981), pp. 208–215, 224–225, 230–245, and 344–355.
2. B. Duling and R. M. Berne, *Circ. Res.* **27**, 669 (1970); A. S. Popel, R. N. Pittman, L. Ellsworth [erratum, *Am. J. Physiol.* **261** (September 1991)] *ibid.* **256**, H921 (1989); D. P. Swain and R. N. Pittman, *ibid*., p. H247; I. Torres Filho, H. Kerger, M. Intaglietta, *Microvasc. Res.* **51**, 202 (1996); D. Buerk, R. Shonat, C. Riva, S. Cranstoun, *ibid.* **45**, 134 (1993).
3. M. Intaglietta, P. Johnson, R. Winslow, *Cardiovasc. Res.* **32**, 632 (1996); E. Braunwald, Ed., *Heart Disease: A Textbook of Cardiovascular Medicine* (Saunders, Philadelphia, PA, 1988); E. Antonini and M. Brunori, *Hemoglobin and Myoglobin in Their Reactions with Ligands* (Elsevier, New York, 1971).
4. M. F. Perutz, in *Molecular Basis of Blood Diseases*, G. Stammatayanopoulos, Ed. (Saunders, Philadelphia, PA, 1987), pp. 127–178; D. Voet and J. G. Voet, (Wiley, New York, 1995), pp. 215–235.
5. L. Jia, C. Bonaventura, J. Bonaventura, J. S. Stamler, *Nature* **380**, 221 (1996).
6. A. C. Guyton, in *Textbook of Medical Physiology* (Saunders, Philadelphia, PA, 1981), pp. 504–513.
7. Methods of the ring bioassay can be found in J. S. Stamler *et al*., *Proc. Natl. Acad. Sci. U.S.A.* **89**, 444 (1992). PO_2 was measured as described in (*11*). Attempts were made to achieve equivalent baseline tone at the different PO_2's by varying the concentration of phenylephrine. SNO–oxy Hb (SNO-Hb[FeII]O_2) and GSNO preparations were synthe-

sized and quantified as described in (*5*).
8. J. S. Stamler *et al*., data not shown.
9. SNO-RBCs (~1 μM) caused 32.5 ± 1.2% relaxation that lasted 14.5 ± 0.7 min in 95% O_2 versus 61 ± 10% relaxation that lasted 23 ± 2 min in <1% O_2 (n = 3 to 4; $P < 0.05$). SNO-RBCs (~0.1 μM) produced small relaxations in <1% O_2 and small contractions in 95% O_2. In contrast, RBCs containing no SNO-Hb produced small contractions (less than those of cell-free Hb) that were potentiated by hypoxia (13 ± 2.0% in 95% O_2 versus 25 ± 5% in <1% O_2; $P <$ 0.05).
10. Protein modeling was done with SYBYL software from TRIPOS Inc. (St. Louis, MO). Hemoglobin coordinates came from the Brookhaven Protein Data Bank (PDB): In oxy Hb, 1HCO and other PDB coordinate files; in deoxy Hb, 3HHB and other PDB files. NO was modeled onto oxy Hb and deoxy Hb with the use of the bond distances and angles recorded in S. Oae and K. Shinhama [*Org. Prep. Proc. Int.* **15**, 165 (1983)] with rotational freedom about the Cα–Cβ, Cβ, Cβ–Sγ, Sγ–Nδ bonds. Figures were prepared with the program VIEW (L. Bergman, University of North Carolina).
11. Adult Sprague-Dawley rats (290 to 350 g) were anesthetized with sodium pentobarbital, intubated, and ventilated with a respirator to maintain the arterial CO_2 pressure at 35 to 45 mmHg. Drugs were infused through the femoral vein, and blood pressure was monitored via the femoral artery as described in (*5*). Blood gas tensions and pH were measured periodically; the blood was replaced with three volumes of 0.9% saline. The tissue PO_2 was measured with platinum microelectrodes (50 μm outer diameter, coated with Nafion) implanted stereotaxically in the right and left hippocampus (AP, −3.4 mm; ML, +2.2 mm), caudate putamen nucleus (CPN), and substantia nigra (SN) (see coordinates below) as described in C. A. Piantadosi *et al*., *Free Rad. Biol. Med.* **22**, 725 (1997). The PO_2 electrodes were polarized to −0.65 V against an Ag/AgCl reference, and the current was measured with a low-impedance nanoampere meter. Arterial PO_2 was adjusted by changing the inspired O_2 concentration and atmospheric pressure. Hydrogen (H_2)-sensitive platinum microelectrodes were implanted stereotaxically in the SN (AP, −5.3 mm; ML, −2.4 mm to the bregma, depth 3.2 mm), CPN (AP, +0.8 mm; ML, −2.5 mm, depth 5.2 mm), and parietal cortex, for measurement of regional blood flow. The microelectrodes were insulated with epoxy, with the exception of the Nafion-coated tip (1 mm). The electrodes were polarized to 400 mV against a reference electrode, and the current was measured with a low-impedance nanoampere meter during and after the inhalation of hydrogen gas (2.5%) for 1 min. The H_2-clearance curves and O_2 tracings were recorded with PC WINDAQ (software, DI-200 AC; DATA Q Instruments, OH). Cerebral blood flow was calculated with the initial slope method [W. D. Heiss and H. Traupe, *Stroke* **12**, 161 (1981); W. Young, *ibid.* **11**, 552 (1980)]. Regional blood flow was monitored for 30 min before and after drug administration (time 0).
12. P. M. Tibbles and J. S. Edelsberg, *N. Engl. J. Med.* **334**, 1642 (1996).
13. Approximately 0.1 μM SNO-RBCs lowered blood pressure by 7 ± 1 mmHg and ~0.5 μM SNO-RBCs lowered blood pressure by 16 ± 2 mmHg (n = 8; P < 0.001 versus baseline).
14. M. W. Dewhirst, T. W. Secomb, E. T. Ong, R. Hsu, J. F. Gross, *Cancer Res.* **54**, 3333 (1994); H. Kerger, I. Torres Filho, M. Rivas, R. Winslow, M. Intaglietta, *Am. J. Physiol.* **268**, H802 (1995).
15. K. H. Park, L. E. Rubin, S. S. Gross, R. Levi, *Circ. Res.* **71**, 992 (1992); V. Hampl, S. L. Archer, D. P. Nelson, E. K. Weir, *J. Appl. Physiol.* **75**, 1748 (1993).
16. M. Casadevall *et al*., *Gastroenterology* **110**, 1156 (1996); S.-M. Kasper *et al*., *Anesth. Analg.* **83**, 921 (1996); J. S. Stamler, *Nature* **380**, 108 (1996); M. G. Persson, L. E. Gustafsson, N. P. Wiklund, P. Hedqvist, S. Moncada, *Br. J. Pharmacol.* **100**, 463 (1990); D. Mitchell and K. Tyml, *Am. J. Physiol.* **270** (*Heart Circ. Physiol.* **39**), H1696 (1996); C. E. King *et al*., *J. Appl. Physiol.* **76**, 1166 (1994).
17. We are indebted to M. Dewhirst for his insight. J.S.S. is a Pew scholar in the biomedical sciences and the recipient of grants from the National Heart, Lung, and Blood Institute (NHLBI) (HL 52529 and HR59130). C.A.P. is funded by the NHLBI.

17 January 1997; accepted 2 May 1997

In Vivo Endoscopic Optical Biopsy with Optical Coherence Tomography

Guillermo J. Tearney, Mark E. Brezinski,* Brett E. Bouma, Stephen A. Boppart, Costas Pitris, James F. Southern, James G. Fujimoto

Current medical imaging technologies allow visualization of tissue anatomy in the human body at resolutions ranging from 100 micrometers to 1 millimeter. These technologies are generally not sensitive enough to detect early-stage tissue abnormalities associated with diseases such as cancer and atherosclerosis, which require micrometer-scale resolution. Here, optical coherence tomography was adapted to allow high-speed visualization of tissue in a living animal with a catheter-endoscope 1 millimeter in diameter. This method, referred to as "optical biopsy," was used to obtain cross-sectional images of the rabbit gastrointestinal and respiratory tracts at 10-micrometer resolution.

Medical imaging technology has advanced over the last 20 years to provide physicians with indispensable information on the macroscopic anatomy of patients. Imaging techniques such as conventional x-ray radiography, magnetic resonance imaging, computed tomography, and ultrasonography have allowed the noninvasive investigation of large-scale structures in the human body with resolutions ranging from 100 μm to 1 mm. However, this resolution is insufficient for the identification of many important pathologies, such as early neoplastic changes or coronary atherosclerotic plaques predisposed to rupture. Identification of these abnormalities requires technologies that resolve clinically relevant tissue microstructure in the range of conventional biopsy.

Optical coherence tomography (OCT) is an optical imaging technique that allows high-resolution cross-sectional imaging of tissue microstructure (*1*). OCT is analogous to ultrasound imaging except that infrared light waves rather than acoustic waves are used. An optical beam is focused into the tissue, and the echo time delay of light reflected from internal microstructure at different depths is measured by interferometry. Image information is obtained by performing repeated axial measurements at different transverse positions as the optical beam is scanned across the tissue. The resulting data constitute a two-dimensional map of the backscattering or reflectance from internal architectural morphology and cellular structures in the tissue.

OCT is attractive for clinical imaging for three reasons. (i) The typical OCT image has an axial resolution of 10 μm, up to 10 times higher than any clinically available diagnostic imaging modality. (ii) Because OCT systems can be constructed with fiber optical components used in telecommunications, they are relatively inexpensive and portable. (iii) Fiber optic systems can be incorporated into catheters or endoscopes, allowing high-resolution images of internal organ microstructure.

Initially, OCT was applied to imaging the transparent tissue of the eye (*2*, *3*). Clinical studies have shown that OCT provides high-resolution cross-sectional images of a wide range of retinal macular diseases (*4*, *5*). Recently, imaging to depths of 2 to 3 mm in nontransparent tissue was achieved by use of longer wavelengths in the near infrared (*1*, *6*–*9*). The identification of in vitro pathology has been verified in tissue from the cardiovascular system and gastrointestinal tract (*8*, *10*).

Here we demonstrate in vivo endoscope-based OCT imaging of the gastrointestinal and respiratory tracts of a rabbit at an axial resolution of 10 μm. To achieve this resolution, we constructed an OCT system that uses a light source with appropriate power and wavelength characteristics, a high-speed optical delay line based on femtosecond pulse shaping, and a second-generation

G. J. Tearney, B. E. Bouma, S. A. Boppart, C. Pitris, J. G. Fujimoto, Department of Electrical Engineering and Computer Science and Research Laboratory of Electronics, Building 36-357, Massachusetts Institute of Technology, 77 Massachusetts Avenue, Cambridge, MA 02139, USA. M. E. Brezinski, Cardiac Unit, Massachusetts General Hospital (Harvard Medical School), Knight Catheterization Laboratory, Fruit Street, Boston, MA 02114, USA. J. F. Southern, Department of Pathology, Sinai Samaritan Hospital, Milwaukee, WI 53233, USA.

*To whom correspondence should be addressed at Building 36-357, Massachusetts Institute of Technology, 77 Massachusetts Avenue, Cambridge, MA 02139, USA. E-mail: mebrezin@mit.edu